Earthline Journal of Chemical Sciences
E-ISSN: 2581-9003; CODEN: EJCSB4
Volume 11, Number 4, 2024, Pages 515-537
https://doi.org/10.34198/ejcs.11424.515537

Luminol tautomers and their interaction with zinc cation – A DFT treatment

Lemi Türker

Department of Chemistry, Middle East Technical University, Üniversiteler, Eskişehir Yolu No: 1, 06800 Çankaya/Ankara, Turkey; e-mail: lturker@gmail.com; lturker@metu.edu.tr

Abstract

Luminol is a chemiluminescent material having variety of applications. In the present study, its 1,3-proton tautomers have been considered within the restrictions of density functional theory at the level of B3LYP/6-31++G(d,p) and B3LYP/6-311++G(d,p) levels. Also, interaction of luminol tautomers with zinc dication at the level of B3LYP/6-31++G(d,p) is considered. All the structures considered presently are thermally favored and electronically stable at the standard states. The effect of zinc dication on the tautomers of luminol is not drastic but causes some conformational changes and enhancing the hydrogen bond formation in some cases. Some electron population has been transferred from the organic partner of the composite to the zinc cation, thereby lowering the initial formal charge of the cation. Various structural and quantum chemical data have been collected and discussed, including IR and UV-VIS spectra. Also the NICS (0) data have been obtained for the tautomers.

1. Introduction

Over the last decades luminol has become one of the widest used chemiluminescent reagent for application to molecular biology and analytical chemistry [1]. It has been used as the basis for a multitude of sensitive and selective detection methods including high performance liquid chromatography (HPLC), immunoassay, DNA probes, DNA typing and as substrate in western blot detection [2-10]. More recently, also historical and archaeological studies using luminol have been successfully carried out [11,12] disclosing an interesting new application field for luminol-based assays.

Received: August 6, 2024; Accepted: September 2, 2024; Published: September 10, 2024

Keywords and phrases: luminol; tautomers; zinc cation; density functional; NICS.

Although there is some debate about the first report of the synthesis of luminol, Schmitz has often been suggested as the first one who has produced luminol in 1908 [13]. The chemiluminescence property of luminol was first discovered by Albrecht in 1928 [14].

Luminol is a strong chemiluminescent compound (the energy released as a photon comes directly from a strong exothermic reaction) characterized by blue light emission upon oxidative conditions. The process itself is quite useful and attractive, especially for analytical applications. In 1928 a forensic scientist, Specht, was the one who first studied in depth the role of hemin, an iron-containing compound derived from heme, in the chemical reaction involving luminol [14]. He investigated its potential application in blood detection [15]. This was the first use of liquid phase chemiluminescence for analytical purposes. Investigating both the chemical structure and reaction properties of luminol, Proesher and Moody correctly predicted the keto-enolic tautomerisation of luminol in alkaline solutions and the fully protonated form in acidic solutions [16].

McGrath evaluated the specificity of the luminol test on biological fluids and showed that luminol displayed a specificity for blood while appearing insensitive to the other biological fluids studied [17].

Grodsky et al., [18] proposed a blend of powders made up of luminol, sodium carbonate (Na_2CO_3) and sodium perborate ($NaBO_3 \cdot nH_2O$) mixed with distilled water. This subsequently became the formula that is most commonly used by today's investigators to detect traces of blood at the site of a crime. An alternative formulation was proposed by Weber which includes luminol, sodium hydroxide or potassium hydroxide, and hydrogen peroxide diluted in distilled water [19].

Upon suitable conditions (that typically include an oxidant species and alkaline media), luminol is oxidized to aminodiphthalate [20]. Although, many reaction pathways can occur but to have light emission, the reaction should proceed in such a way that when the aminodiphthalate is formed, it is in an electronic excited state, that will then return to its ground state, possibly accompanied with light emission. The formation of that excited state possibly would be a result from the accumulation of the energy in one of the chemical species formed in an extremely exothermic reaction step [20].

Luminol is used to detect the blood effects at the crime scene by the police or the forensic team, where they are present at the crime scene, lights are turned off and glare is detected. However, the bad thing is that they might destroy other evidence at the crime

scene. For this reason, it is used by forensic investigators after other evidence is explored and is not used by many police officers to protect material evidence. For this reason scientists have been able to develop new techniques that can replace luminol [21]. Luminol and some of its derivatives have been studied extensively and used in many applications [22-31].

The presence of electron donating substituents altered the electronic properties of the luminol and this phenomenon was evaluated in relation to the chemiluminescence potential of the studied disubstituted luminol derivatives [30,31]. To investigate the molecular basis of the chemiluminescence mechanism of luminol, molecular orbital calculations using three different theoretical calculation methods (that is the Restricted Hartree Fork (RHF), Density Functional Theory (DFT) with hybrid function of Becke three-parameters Lee, Yang and Parr (B3LYP), and Møller-Plesset Perturbation Theory (MP2)) have been done [30,31]. Different behavior was observed for the studied molecular structures in different phases (gas, water, and dimethylformamide) to emphasize the influence of molecular environment on the chemiluminescence property, regardless of the theoretical methods employed. It has been observed that the electron donating moiety induced better chemiluminescence property depending on the donating power, position as well as the number of such substituents [31].

Yue and Liu investigated the mechanistic of pH-dependent luminol chemiluminescence in aqueous solution [32]. Effect of hydrogen bonding solvent on excited-state properties of luminol was searched by Moyon and coworkers [33].

In the present study, 1,3-proton tautomers of luminol and their interaction with zinc dication have been considered within the constraints of density functional theory. Also, NICS(0), calculations have been carried out for the 6-memebered rings of the luminol tautomers having cyclic conjugation.

2. Method of Calculation

In the present study, the initial optimizations of all the structures leading to energy minima have been achieved by using molecular mechanics (MM2) method followed by semi-empirical PM3 self-consistent fields molecular orbital (SCF MO) method [34,35] at the restricted level [36,37]. Subsequent optimizations were achieved at Hartree-Fock level using various basis sets. Then, the structural optimizations were managed within the framework of density functional theory (DFT) [38,39] at the levels of B3LYP/6-

31++G(d,p) [37,40] and B3LYP/6-311++G(d,p) for the tautomers. Whereas, for the zinc dication composites of the tautomers B3LYP/6-31++G(d,p) level of calculations have been performed because the former basis set does not have parameterization for zinc atom. Note that the exchange term of B3LYP consists of hybrid Hartree-Fock and local spin density (LSD) exchange functions with Becke's gradient correlation to LSD exchange [39,41]. The correlation term of B3LYP consists of the Vosko, Wilk, Nusair (VWN3) local correlation functional [42] and Lee, Yang, Parr (LYP) correlation correction functional [43]. Also, the vibrational analyses have been carried out. The total electronic energies are corrected for the zero point vibrational energy (ZPE). The normal mode analysis for each structure yielded no imaginary frequencies for the $3N–6$ vibrational degrees of freedom, where N is the number of atoms in the system. This indicates that the structure of each molecule corresponds to at least a local minimum on the potential energy surface. All these calculations were done by using the Spartan 06 package program [44]. Whereas the nucleus-independent chemical shift, NICS(0), calculations have been performed by using Gaussian 03 program [45].

3. Results and Discussion

Luminol tautomers

The 1,3-proton tautomers of luminol are named as luminol-A, luminol-B, etc. Figures 1 and 2 show the optimized structures of luminol tautomers at different level of calculations. The figures also show the direction of the dipole moment vectors and possible hydrogen bonding cites. In the figures, note the direction of the dipole moment vector and the conformations of the OH groups in luminol-B at two different levels of the calculations.

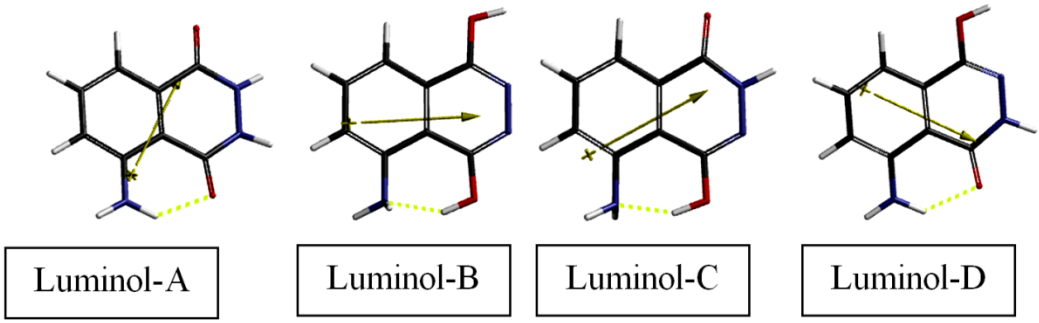

Figure 1. Optimized structures of the tautomers (B3LYP/6-31++G(d,p)).

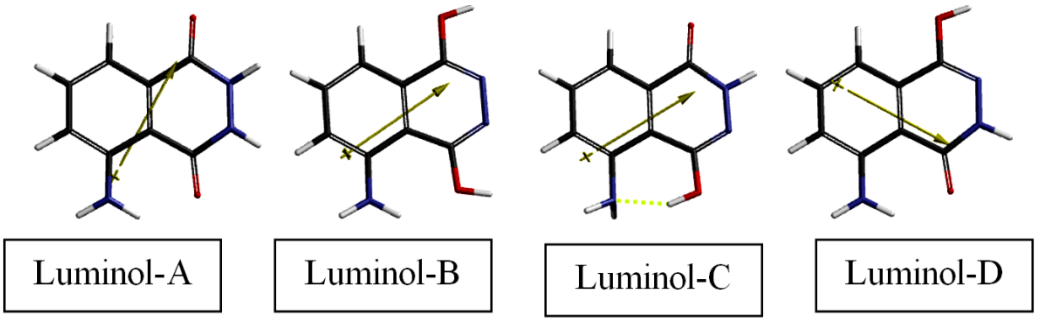

Figure 2. Optimized structures of the tautomers (B3LYP/6-311++G(d,p)).

Tables 1 and 2 include some thermo chemical properties of luminol tautomers at different level of calculations where Hº and Gº stand for the standard heat of formation and the Gibbs free energy of formations.

Table 1. Some thermo chemical properties of the tautomers considered.

Tautomer	Hº	Sº (J/molº)	Gº
Luminol-A	-1637432.129	397.79	-1637550.734
Luminol-B	-1637357.658	393.08	-1637474.854
Luminol-C	-1637405.986	392.10	-1637522.893
Luminol-D	-1637448.693	396.48	-1637566.905

(B3LYP/6-31++G(d,p) level of calculations. Energies in kJ/mol.

Table 2 . Some thermo chemical properties of the tautomers considered.

Tautomer	Hº	Sº (J/molº)	Gº
Luminol-A	-1637794.945	397.22	-1637913.380
Luminol-B	-1637750.820	395.19	-1637868.646
Luminol-C	-1637765.841	392.44	-1637882.850
Luminol-D	-1637809.052	396.22	-1637927.185

(B3LYP/6-311++G(d,p) level of calculations. Energies in kJ/mol.

As seen in Tables 1 and 2, at the standard conditions all the tautomers possess exothermic heat of formation and favorable Gº values irrespective of the level of calculations performed. The algebraic order of Hº and Gº values in both sets of

calculations are luminol-D< luminol-A< luminol-C< luminol-B, respectively. However, for each tautomer B3LYP/6-311++G(d,p) level of calculations predict more exothermic and more favorable values compared to the respective values of B3LYP/6-31++G(d,p) calculations.

Tables 3 and 4 contain some energies of luminol tautomers at different level of calculations, where E, ZPE and E_C stand for the total electronic energy, zero point vibrational energy and the corrected total electronic energy, respectively. As seen in the tables, the tautomers considered are electronically stable, although B3LYP/6-311++G(d,p) level of calculations result more stable tautomers. The algebraic order of E_C values in both cases of the calculations is luminol-D< luminol-A< luminol-C< luminol-B.

Table 3. Some energies of the tautomers considered.

Tautomer	E	ZPE	E_C
Luminol-A	-1637837.92	393.26	-1637444.66
Luminol-B	-1637762.38	393.05	-1637369.33
Luminol-C	-1637812.48	395.06	-1637417.42
Luminol-D	-1637853.73	392.71	-1637461.02

(B3LYP/6-31++G(d,p) level of calculations. Energies in kJ/mol.

Table 4. Some energies of the tautomers considered.

Tautomer	E	ZPE	E_C
Luminol-A	-1638199.82	392.39	-1637807.43
Luminol-B	-1638153.94	390.67	-1637763.27
Luminol-C	-1638171.42	394.07	-1637777.35
Luminol-D	-1638213.60	392.17	-1637821.43

(B3LYP/6-311++G(d,p) level of calculations. Energies in kJ/mol.

Figure 3 displays the ESP charges on the atoms of tautomers considered and theirs electrostatic potential maps where negative potential regions reside on red/reddish and positive ones on blue/bluish parts of the maps. Note that the ESP charges are obtained by the program based on a numerical method that generates charges that reproduce the electrostatic potential field from the entire wavefunction [44].

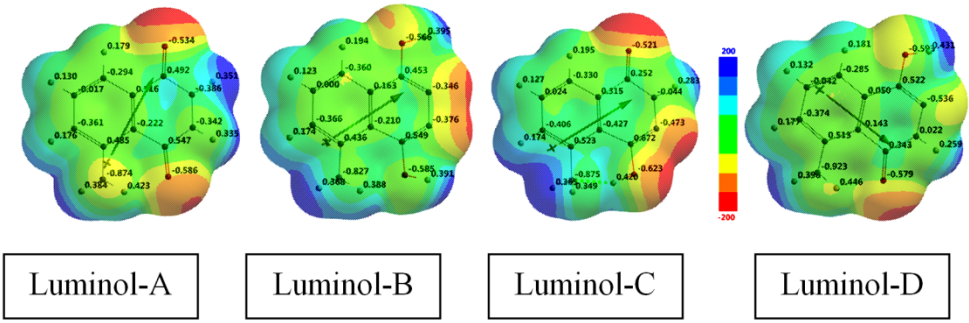

Figure 3. The ESP charges on the atoms of tautomers considered and theirs electrostatic potential maps (B3LYP/6-311++G(d,p) level of calculations).

Table 5 shows some calculated properties of the tautomers considered. The dipole moments show some noticeable fluctuations from one tautomer to the other. Obviously, various structural, electronic and hydrogen bonding variations are responsible for it.

Table 5. Some calculated properties of the tautomers considered.

Tautomer	Dipole Moment	Polarizability	Area (Å²)	Volume (Å³)	PSA (Å²)	Log P
Luminol-A	2.19	53.45	178.16	161.00	76.884	-2.56
Luminol-B	3.59	53.37	177.52	160.58	78.058	-0.82
Luminol-C	6.64	53.40	177.89	160.82	76.803	-1.69
Luminol-D	1.91	53.40	177.56	160.56	76.877	-1.69

B3LYP/6-311++G(d,p) level of calculations. Dipole moments in Debye units. Polarizabilities in 10^{-30} m^3 units. All have ovality of 1.24.

It is worth mentioning that the polar surface area (PSA) is defined as the amount of molecular surface area arising from polar atoms (N,O) together with their attached hydrogen atoms. Although these compounds are isomeric, their PSA values differ from each other meaning that the same kind of atoms might be influenced by electronic factors differently at different positions.

As for the log P values, note that a negative value for log P means the compound has a higher affinity for the aqueous phase (it is more hydrophilic); when log P = 0 the compound is equally partitioned between the lipid and aqueous phases; whereas a positive value for log P denotes a higher concentration in the lipid phase (i.e., the compound is more lipophilic).

Table 6 shows the aqueous (E_{aq}) and solvation energies (E_{solv}) for the tautomers considered. The algebraic order of aqueous energies is luminol-C < luminol-D < luminol-A < luminol-B. On the other hand, the solvation energies follow the order of luminol-C < luminol-B < luminol-D < luminol-A. These orders are dictated by the presence of various chemical functional descriptors and their variations as going from one tautomer to the other or from one isomer to the other.

Table 6. Aqueous and solvation energies for the tautomers considered.

	Luminol-A	Luminol-B	Luminol-C	Luminol-D
E_{aq}	-1638249.80	-1638221.20	-1638389.20	-1638268.77
E_{solv}	-49.983	-67.264	-217.783	-55.170

Based on B3LYP/6-311++G(d,p) level of optimization. Energies in kJ/mol. SM5.4/A model used for solvation energy.

Figure 4 shows the chemical function descriptors (CFDs) of the tautomers considered. In the figure green spheres stand for hydrogen bond acceptors; bluish ones for hydrophobe; the purple for hydrogen bond donor, acceptor and ionizable sites; whereas yellowish ones indicate hydrogen bond acceptors and donors in character.

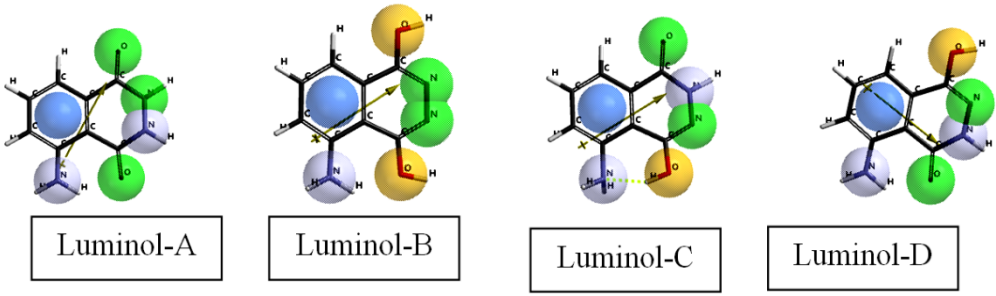

Figure 4. CFDs of the tautomers considered (B3LYP/6-311++G(d,p)) .

The calculated (B3LYP/6-31++G(d,p)) IR spectrum of luminol-A has asymmetric HN-H stretching at 3713 cm^{-1} whereas the symmetrical one occurs at 3523 cm^{-1}. The N-H stretching of the ring are at 3587 cm^{-1} and 3589 cm^{-1}. The IR spectrum of luminol-B possesses HN-H stretching (asymmetrical) at 3587 cm^{-1}. The O-H stretchings occur at 3757 cm^{-1}, 3490 cm^{-1} (coupled with H-NH stretching) and 3451 cm^{-1}. The HN-H stretching (asymmetrical) of luminol-C happens at 3583 cm^{-1} and 3492 cm^{-1}. The stretching at 3617 cm^{-1} belongs to the ring N-H whereas O-H stretching is at 3551 cm^{-1}.

As for luminol-D spectrum, the HN-H stretchings are at 3721 cm^{-1} and 3510 cm^{-1}. The ring N-H stretching occurs at 3629 cm^{-1} whereas the O-H stretching is at 3788 cm^{-1}.

Tables 7 and 8 show the HOMO, LUMO energies and the interfrontier molecular orbital energy gap, Δε, values ($\Delta\varepsilon=\varepsilon_{LUMO}-\varepsilon_{HOMO}$) of the tautomers considered at different level of calculations.

Table 7. The HOMO, LUMO energies and Δε values of the tautomers considered.

Tautomer	HOMO	LUMO	Δε
Luminol-A	-591.511162	-193.651551	397.859611
Luminol-B	-599.760804	-173.533069	426.227735
Luminol-C	-592.500201	-180.452458	412.047743
Luminol-D	-565.440197	-160.861686	404.578511

(B3LYP/6-31++G(d,p)) level of calculations. Energies in kJ/mol.

Table 8. The HOMO, LUMO energies and Δε values of the tautomers considered.

Tautomer	HOMO	LUMO	Δε
Luminol-A	-596.891604	-196.232214	400.659390
Luminol-B	-566.294622	-145.856729	420.437893
Luminol-C	-599.047239	-185.296237	413.751002
Luminol-D	-571.674643	-165.185928	406.488715

(B3LYP/6-311++G(d,p)) level of calculations. Energies in kJ/mol.

The algebraic order of the HOMO energies are luminol-B< luminol-C<luminol-A< luminol-D (B3LYP/6-31++G(d,p)) whereas B3LYP/6-311++G(d,p) level of calculations yield the order as luminol-C< luminol-A< luminol-D< luminol-B. As for the orders of the LUMO energies, they are luminol-A< luminol-C< luminol-B< luminol-D and luminol-A< luminol-C< luminol-D< luminol-B, respectively for the B3LYP/6-31++G(d,p) and B3LYP/6-311++G(d,p) level of calculations. Although, the orders of the HOMO and LUMO energies differ depending on the level of calculation, the order of Δε, values are the same that is luminol-A< luminol-D< luminol-C< luminol-C< luminol-B. All these

orders arise from some intricate and implicit functions of various factors including the optimization as the main one.

Figure 5 shows the local ionization potential maps of the tautomers considered where conventionally red/reddish regions (if any exists) on the density surface indicate areas from which electron removal is relatively easy, meaning that they are subject to electrophilic attack. It is worth remembering that the local ionization potential map is a graph of the value of the local ionization potential on an isodensity surface corresponding to a van der Waals surface.

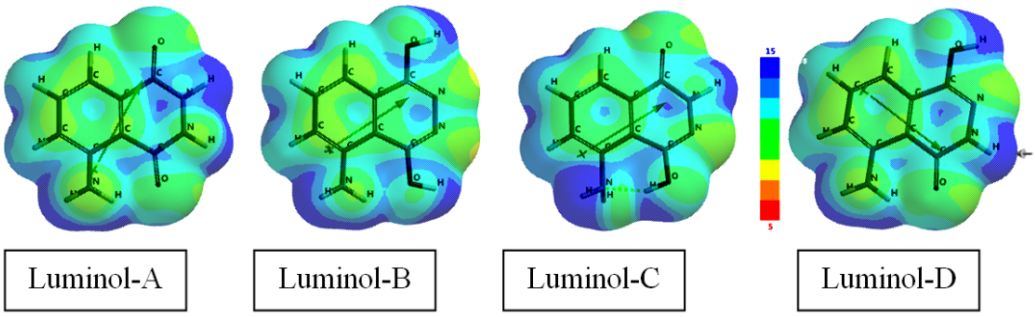

Figure 5. The local ionization potential maps of the tautomers considered (B3LYP/6-311++G(d,p)) level of calculations.

Figure 6 displays the LUMO maps of the isomers considered. Note that a LUMO map displays the absolute value of the LUMO on the electron density surface. The blue color (if any exists) stands for the maximum value of the LUMO and the red colored

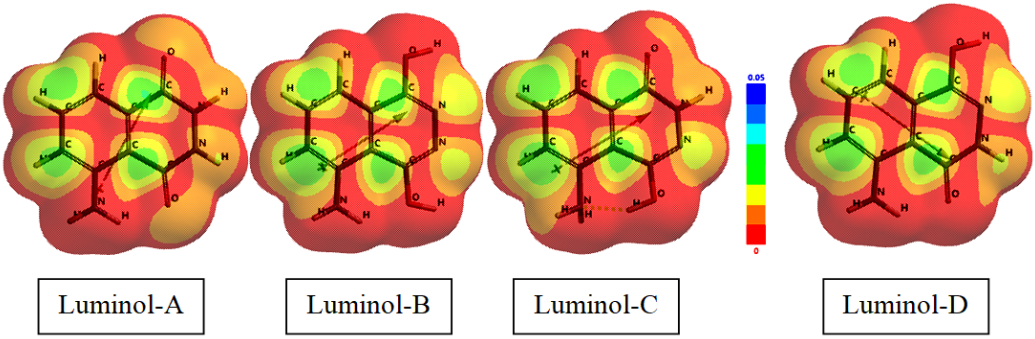

Figure 6. The LUMO maps of the tautomers (B3LYP/6-311++G(d,p)) level of calculations.

region, associates with the minimum value. Note that the LUMO and NEXTLUMO are the major orbitals directing the molecule towards of the attack of nucleophiles [44]. Positions where the greatest LUMO coefficient exists is the most vulnerable site in nucleophilic reactions.

Figure 7 shows the time-dependent density functional (TDDFT) UV-VIS spectra of the isomers. As seen in the figure, they all absorb in the UV region having almost no absorbance in the visible part. The occurrence of tautomerism in luminol-A, producing luminol-B extends the π-conjugation, and the heterocyclic ring becomes aromatic (NICS(0) value of the heterocyclic ring is -5.70). In the cases of luminol-C and Luminol-D, two λ_{max} values happen due to overlapped peaks. Since the calculated spectra involve not only the HOMO-LUMO excitations, some of the spectra possess shoulders or overlapped peaks.

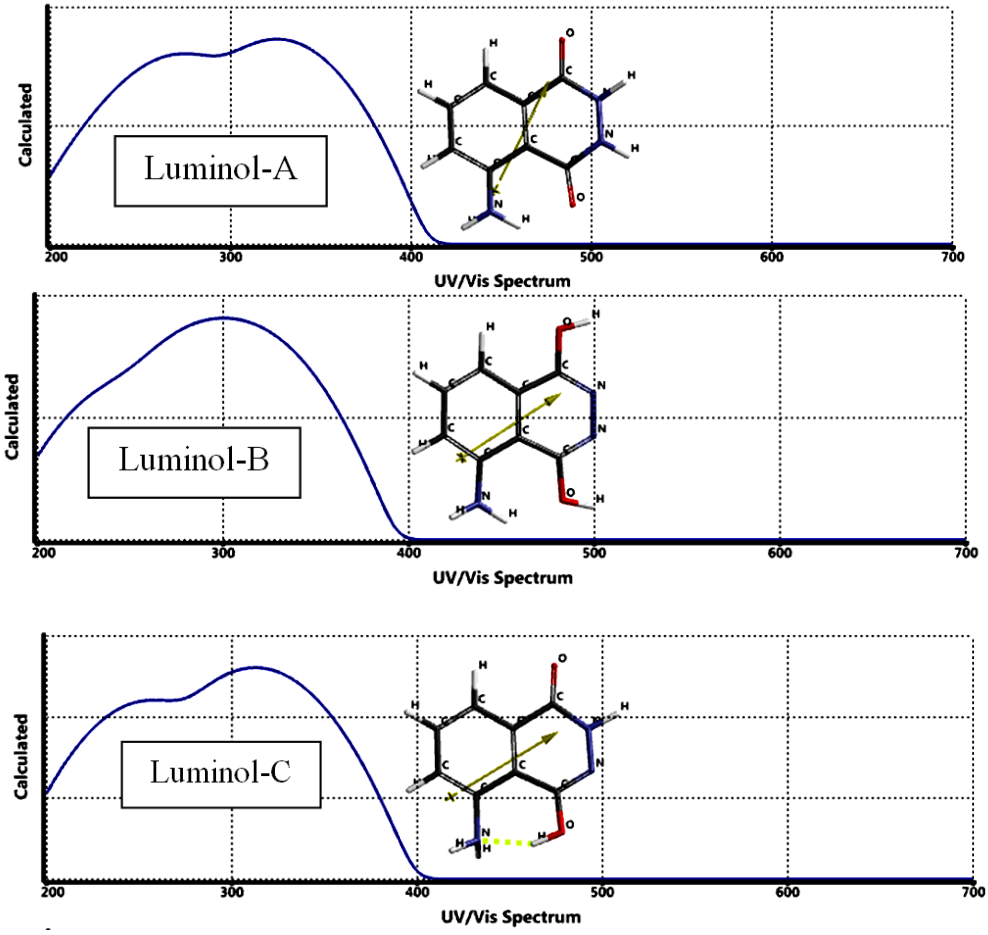

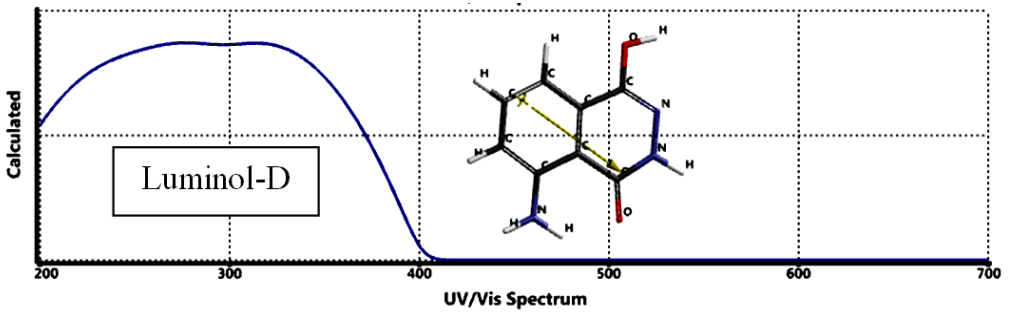

Figure 7. The time-dependent density functional UV-VIS spectra of the tautomers.

Table 9 lists the NICS(0) value of the carbocyclic ring of luminol tautomers presently considered. The respective value of the heterocyclic ring in luminol-B is -5.70. The variation of the data in Table 9 arises from the effect of substituent(s) on the ring current of the carbocyclic ring so that the aromaticity order turns out to be luminol-A<luminol-D< luminol-B< luminol-C.

Table 9. The NICS(0) values of the carbocyclic ring of luminol tautomers.

Luminol-A	Luminol-B	Luminol-C	Luminol-D
-7.53	-8.42	-9.45	-7.81

B3LYP/6-311++G(d,p) level.

The interaction with zinc cation

In this part of the study, computations are at the level of B3LYP/6-31++G(d,p). Figure 8 shows the optimized structures of the composite tautomers considered. As seen in the figure, the O-H bonds in luminol-B+Zn^{+2} and luminol-C+Zn^{+2} are noticeably elongated in the presence of the zinc cation. Probably some interaction occurs between the cation and oxygen atom (charge-lone-pair interaction) of the OH group which weakens the strength of the O-H bond, thus assisting formation of the hydrogen bond with the nitrogen atom forming a six-membered quasi-ring.

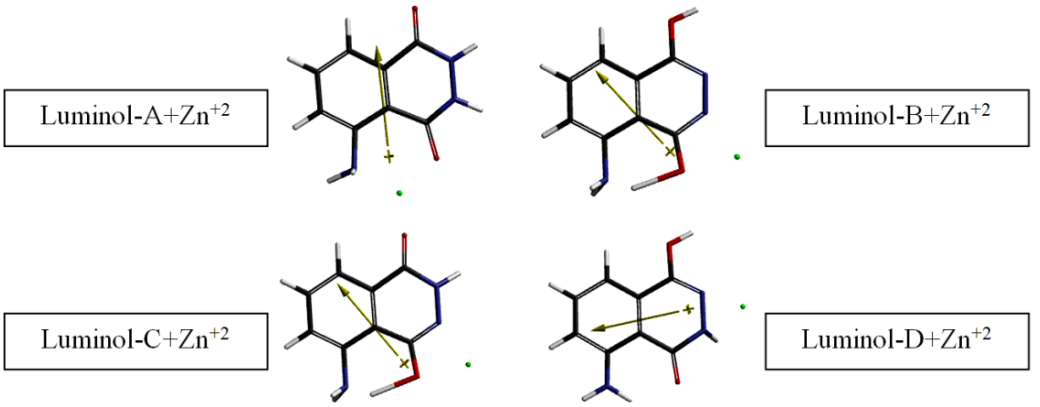

Figure 8. Optimized structures of the composite tautomers.

Tables 10 and 11 show some thermo chemical properties and some energies of the composite tautomers, respectively. As seen in the table all the composite tautomers possess exothermic heat of formation values and favorable Gibbs free energy of formation values at the standard state. The algebraic orders of Hº and Gº values are the same that is luminol-B+Zn^{+2}<luminol-A+Zn^{+2}< luminol-C+Zn^{+2}< luminol-D+Zn^{+2}.

Table 10. Some thermo chemical properties of the composite tautomers considered.

Composite tautomer	Hº	Sº (J/molº)	Gº
Luminol-A+Zn^{+2}	-6306895.864	419.49	-6307020.944
Luminol-B+Zn^{+2}	-6306896.861	423.15	-6307023.018
Luminol-C+Zn^{+2}	-6306859.421	425.64	-6306986.313
Luminol-D+Zn^{+2}	-6306723.262	423.80	-6306849.628

Energies in kJ/mol.

The data presented in Table 11 reveals that the composite tautomers are all electronically stable and the stability order is luminol-B+Zn^{+2}> luminol-A+Zn^{+2}> luminol-C+Zn^{+2}> luminol-D+Zn^{+2}.

Table 11. Some energies of the composite tautomers considered.

Composite tautomer	E	ZPE	E_C
Luminol-A+Zn^{+2}	-6307268.60	401.66	-6306866.94
Luminol-B+Zn^{+2}	-6307270.33	401.71	-6306868.62
Luminol-C+Zn^{+2}	-6307232.61	401.20	-6306831.41
Luminol-D+Zn^{+2}	-6307091.30	396.11	-6306695.19

Energies in kJ/mol.

Figure 9 displays the ESP charges on atoms of the composite tautomers considered.

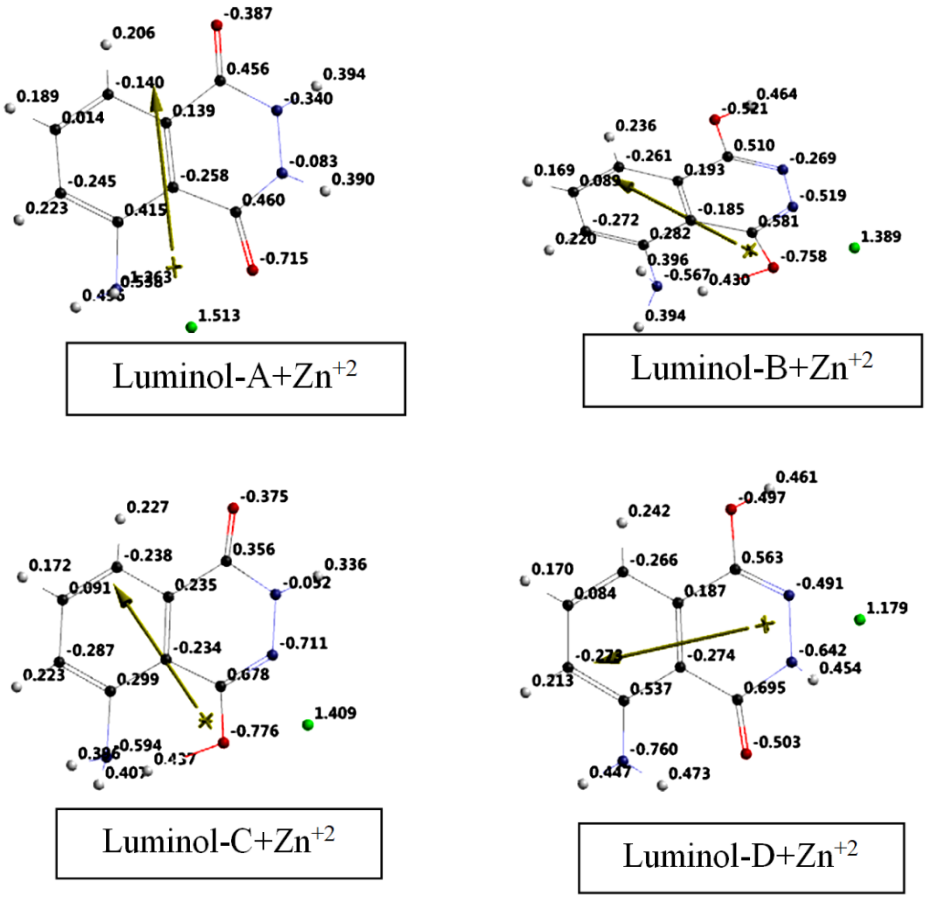

Figure 9. The ESP charges on atoms of the composite tautomers considered.

In the figure one should notice that the initial formal charge of the zinc cation has been decreased in all the composites, implying that some electron population has been transferred from luminol component to the cation.

Figure 10 shows the chemical function descriptors (CFDs) of the composite tautomers considered. In the figure green spheres stand for hydrogen bond acceptors; bluish ones for hydrophobe; the purple: hydrogen bond donor, acceptor and ionizable sites; whereas yellowish ones indicate hydrogen bond acceptors and donors in character. As the tautomerism happens the structural and electronic dictators in the composites change thus the character of chemical function descriptors in the composites vary.

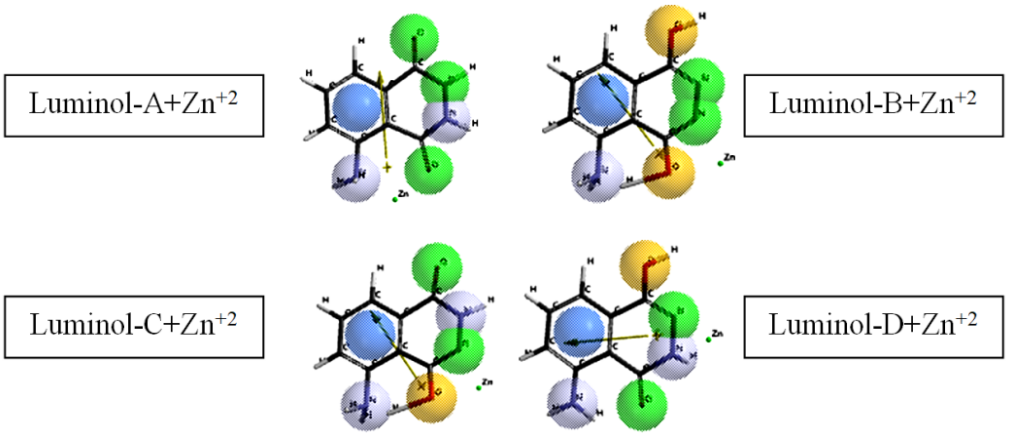

Figure 10. CFDs of the composite tautomers considered.

Table 12 shows some calculated properties of the composite tautomers considered.

Table 12. Some properties of the composite tautomers considered.

Composite tautomer	Dipole Moment	Polarizability	PSA (Å^2)
Luminol-A+Zn^{+2}	16.1234116	54.55	76.333
Luminol-B+Zn^{+2}	13.7204958	54.49	74.478
Luminol-C+Zn^{+2}	16.0039058	54.62	74.266
Luminol-D+Zn^{+2}	12.7186782	54.90	74.173

Dipole moments in Debye units. Polarizabilities in 10^{-30} m^3 units. All have ovality value of 1.28.

Figure 11 shows the LUMO maps of the composite tautomers.

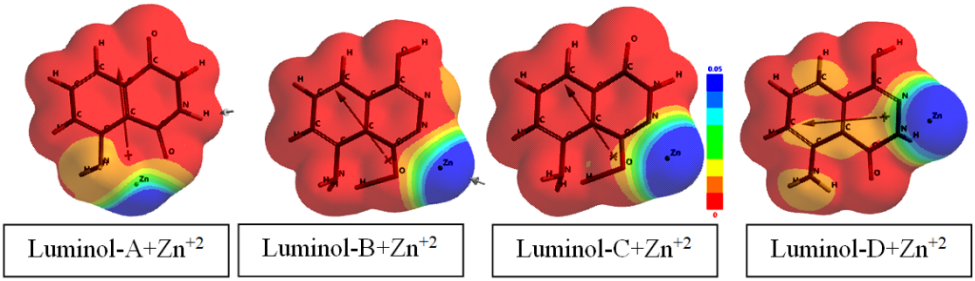

Figure 11. The LUMO maps of the composite tautomers.

Figure 12 displays some of the molecular orbital energy levels of composite tautomers considered. The figure reveals that not only the frontier molecular orbital (FMO) energy levels but also the inner lying molecular orbital energy levels vary from structure to structure. Their distributions dictate the thermal stability of the composites. The determining factors on the energy levels of the inner lying molecular orbitals are structural factors coming from tautomerism as well as the interaction with the zinc cation. As the cation attracts some electron population from the organic moiety, all the molecular orbital energy levels should be lowered down [46] as compared the respective orbital energies of parent tautomers.

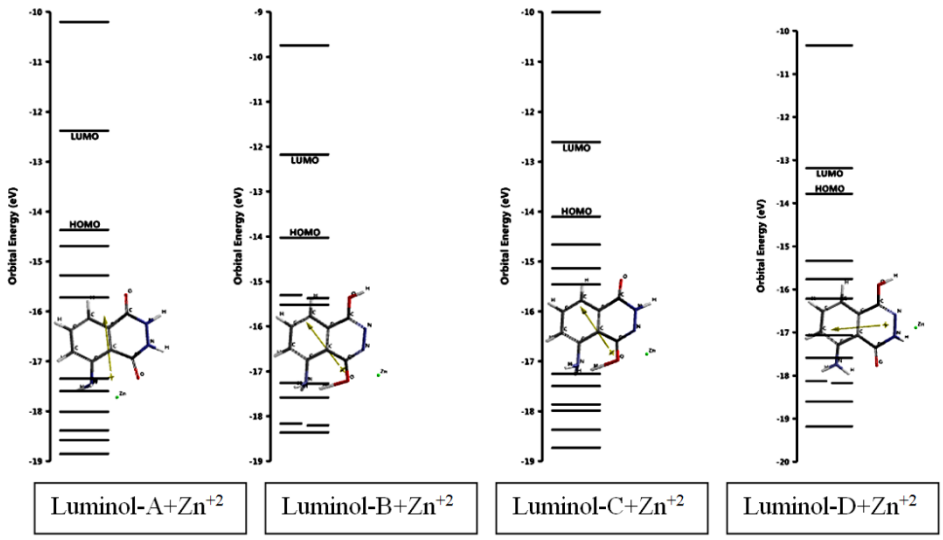

Figure 12. Some of the molecular orbital energy levels of the composite tautomers considered.

Table 13 shows the HOMO, LUMO energies and the interfrontier molecular orbital energy gaps (Δε) of the composites considered, where is $\Delta\varepsilon=\varepsilon_{LUMO}-\varepsilon_{HOMO}$. The algebraic orders of the HOMO and LUMO energies are luminol-A+Zn^{+2}< luminol-C+Zn^{+2}< luminol-B+Zn^{+2}< luminol-D+Zn^{+2} and luminol-D+Zn^{+2}< luminol-C+Zn^{+2}< luminol-A+Zn^{+2}< luminol-B+Zn^{+2}, respectively. Consequently, the order of Δε values is luminol-D+Zn^{+2}< luminol-C+Zn^{+2}< luminol-B+Zn^{+2}< luminol-A+Zn^{+2}.

Table 13. The HOMO, LUMO energies and Δε values of the composite tautomers considered.

Composite tautomer	HOMO	LUMO	Δε
Luminol-A+Zn^{+2}	-1386.151	-1194.251	191.901
Luminol-B+Zn^{+2}	-1353.682	-1174.611	179.070
Luminol-C+Zn^{+2}	-1360.719	-1216.593	144.126
Luminol-D+Zn^{+2}	-1330.002	-1271.667	58.336

Energies in kJ/mol.

Figure 13 shows the UV-VIS spectra (TDDFT) of the composite tautomers. The figure reveals that in the presence of the cation (1:1 composites) the calculated UV-VIS)

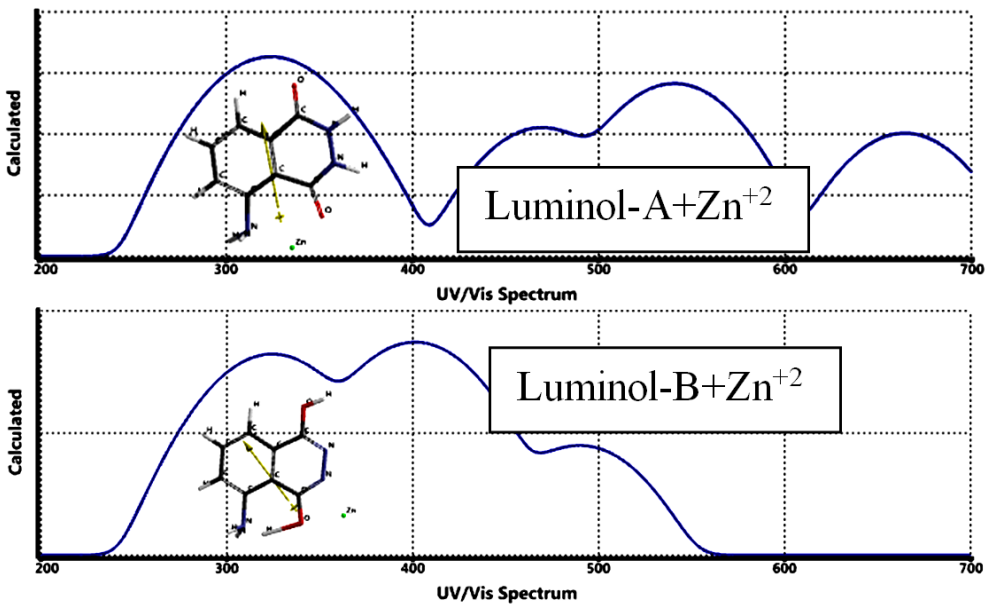

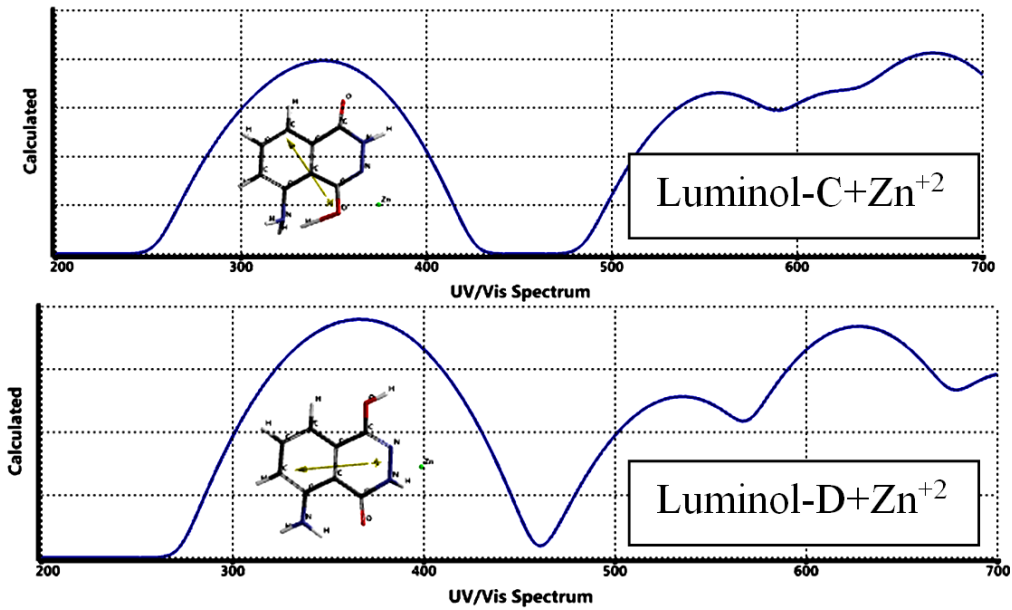

Figure 13. The time-dependent density functional UV-VIS spectra of the composite tautomers considered.

spectra of the tautomers (see Figure 7) are drastically affected in such a way that great bathochromic effect happens and various new absorption peaks emerge in the visible part having different intensities. This effect should arise mainly from the charge of the zinc cation. Note that some electron population has been transferred between the components of the composites. The positive partial charge acquired by the organic component should lower the occupied and the vacant orbitals at unequal extents, thus decreasing the energy gaps for the electronic transitions. The intensities should have been dictated by the magnitudes of the transition moments for the excitations.

4. Conclusion

In the present computational study, luminol and its 1,3-proton tautomers, are considered within the restrictions of density functional theory and the applied basis set(s). In the vacuum conditions, all of them are characterized with exothermic heat of formations and favorable Gibbs free energy of formation values and they are all electronically stable. In the presence of zinc cation the initial formal charge of the zinc cation has been decreased in all the composites, implying that some electron population has been transferred from luminol component to the cation. This effect causes some

accompanying structural and electronic changes as well as improves the hydrogen bond forming tendency and occurrence of appreciable variations in the spectral behavior.

References

[1] Barni, F., Lewis, S.W., Berti, A., Miskelly, G.M., & Lago, G. (2007). Forensic application of the luminol reaction as a presumptive test for latent blood detection. *Talanta 72*(3), 896-913. https://doi.org/10.1016/j.talanta.2006.12.045

[2] Barnett, N.W., & Francis, P.S. (2005). Chemiluminescence: Liquid-phase. *Encyclopedia of Analytical Science* (2nd ed.). London: Elsevier Academic Press. https://doi.org/10.1016/B0-12-369397-7/00070-4

[3] Kricka, L.J., Stanley, P.E., Thorpe, G.H.G., & Whitehead, T.P. (1984). *Proceedings of the 3rd International symposium on bioluminescence and chemiluminescence*. New York: Academic Press.

[4] Nieman, T. (1989). In J.W. Birks (Ed.), *Chemiluminescence and photochemical reaction detection in chromatography* (pp. 99-123). New York: VCH.

[5] García-Campana, A.M., Baeyens, W.R.G., & Zhao, Y. (1997). Peer reviewed: Chemiluminescence detection in capillary electrophoresis. *Anal. Chem., 69*(3), 83A-88A. https://doi.org/10.1021/ac971535m

[6] Yuan, J., & Shiller, A.M. (1999). Determination of subnanomolar levels of hydrogen peroxide in seawater by reagent-injection chemiluminescence detection. *Anal. Chem*., *71*(10), 1975-1980. https://doi.org/10.1021/ac981357c

[7] Roda, A., Pasini, P., Guardigli, M., Baraldini, M., Musiani, M., & Mirasoli, M. (2000). Bio- and chemiluminescence in bioanalysis. *Fresenius J. Anal. Chem*., *366*, 752-759. https://doi.org/10.1007/s002160051569

[8] García-Campana, A.M., & Baeyens, W.R.G. (2001). *Chemiluminescence in analytical chemistry*. Boca Raton: CRC Press. https://doi.org/10.1201/9781482270693

[9] Yamaguchi, M., Yoshida, H., & Nohta, H. (2002). Luminol-type chemiluminescence derivatization reagents for liquid chromatography and capillary electrophoresis. *J. Chromatogr. A*, *950*(1-2), 1-19. https://doi.org/10.1016/S0021-9673(02)00004-3

[10] Barnett, N.W., & Francis, P.S. (2005). Chemiluminescence: Overview. In *Encyclopedia of analytical science* (2nd ed.). London: Elsevier Academic Press. https://doi.org/10.1016/B0-12-369397-7/00069-8

[11] Vish, A.L., & Yeshion, T.E. (2004). The use of luminol as a presumptive blood test for prehistoric archaeological artifacts. *N. Am. Archaeol*., *25*(2), 153-159. https://doi.org/10.2190/XC04-RLF4-NWXT-B7N2

[12] Tug, A., Alakoc, Y.D., & Hanci, I.H. (2005). An end to a rumour. *Forensic Sci. Int*., *153*(2-3), 156-160. https://doi.org/10.1016/j.forsciint.2004.08.022

[13] Schmitz, A.J. (1902). *Ueber das Hydrazid der Trimesinsäure und der Hemimellithsäure*. *Ph.D. Thesis.* Heidelberg University; Heidelberg, Germany.

[14] Albrecht, H.O. (1928). Über die Chemiluminescenz des Aminophthalsäurehydrazids. *Z. Physik. Chem., 136*(614), 321-330. https://doi.org/10.1515/zpch-1928-13625

[15] Specht, W. (1937). Die Chemiluminescenz des Hämins, ein Hilfsmittel zur Auffindung und Erkennung forensisch wichtiger Blutspuren. *Angew. Chem*., *50*(8), 155-157. https://doi.org/10.1002/ange.19370500803

[16] Proescher, F., & Moody, A.M. (1939). Method of detecting and locating traces of blood and a compound for detecting traces of blood. *J. Lab. Clin. Med*., *24*, 1183-1189.

[17] McGrath, J. (1942). Chemical luminescence test for blood. *Br. Med. J., 2*, 156-157. https://doi.org/10.1136/bmj.2.4257.156

[18] Grodsky, M., Wright, K., & Kirk, P.L. (1951). Simplified preliminary blood testing--an improved technique and a comparative study of methods, *J. Crimin. Law Criminol. Police Sci., 42*, 95-104. https://doi.org/10.2307/1140307

[19] Weber, K. (1966). Die Anwendung der chemiluminescenz des luminols in der gerichtlichen medizin und toxikologie: I. Der nachweis von blutspuren. *Dtsch. Z. Gesamte Gerichtl. Med*., *57*, 410-423. https://doi.org/10.1007/BF00583303

[20] Ferreira E.C., & Rossi A.V. (2002). Chemiluminescence as an analytical tool: from the mechanism to applications of the reaction of luminol in kinetic based methods. *Quim. Nova*, *25*(6), 1003-1011. https://doi.org/10.1590/S0100-40422002000600018

[21] Jabarah, Z.A., Mahdi, I.S., & Jaafar, W.A. (2019). Lumonil compounds in criminal chemistry. *Egyptian Journal of Chemistry, 62*(10), 1907-1916. https://doi.org/10.21608/ejchem.2019.9697.1651

[22] Yao, H., Huang, X., Shi, P., Lin, Z., Zhu, M., Liu, A., Lin, X., Tang, Y. (2017). DPPH–luminol chemiluminescence system and its application in the determination of scutellarin in pharmaceutical injections and rat plasma with flow injection analysis. *Luminescence*, *32*, 588-595. https://doi.org/10.1002/bio.3225

[23] Ram, G.S, Vivek M.R., & Maruti L.N. (2013). Effect of temperature on chemiluminescence of luminol ethyl amine in water and DMSO. *Der Chemica Sinica, 4*(3), 161-164.

[24] da Silva, R.R., Agustini, B.C., da Silva, A.L.L., Frigeri, H.R. (2012). Luminol in the forensic science. *Journal of Biotechnology and Biodiversity, 3*(4), 172-177. https://doi.org/10.20873/jbb.uft.cemaf.v3n4.rogiskisilva

[25] Navas, D.A., González G.J.A., & Lovillo, J. (1997). Enhancer effect of fluorescein on the luminol–H_2O_2–horseradish peroxidase chemiluminescence: energy transfer process. *J. Biolumin Chemilumin., 12*, 199-205. https://doi.org/10.1002/(SICI)1099-1271(199707/08)12:4%3C199::AID-BIO445%3E3.0.CO;2-U

[26] Navas, D.A., Sanchez F.G. & Gonzalez, G.J.A. (1998). Phenol derivatives as enhancers and inhibitors of luminol-H_2O_2-horseradish peroxidase chemiluminescence. *J. Biolumin Chemilumin., 13*, 75-84. https://doi.org/10.1002/(SICI)1099-1271(199803/04)13:2%3C75::AID-BIO469%3E3.0.CO;2-7

[27] Li, S.F., Wang, H.Y., Min, X., Zhang, L., Wang, J., Du, J., Zhang, J.Q., Wei, P., Wang, Z.Q., Zhang, H., Wu, W. (2014). Chemiluminescence behavior of luminol-KIO_4-Ag nanoparticles system and its analytical applications. *J. Biomedical Science and Engineering, 7*(6), 307-315. https://doi.org/10.4236/jbise.2014.76033

[28] Khajvand, T., Akhoondi, R., Chaichi, M.J., Rezaee, E., & Golchoubian, H. (2014). Two new dinuclear copper(II) complexes as efficient catalysts of luminol chemiluminescence. *Journal of Photochemistry and Photobiology A: Chemistry, 282*, 9-15. https://doi.org/10.1016/j.jphotochem.2014.02.011

[29] Shinde R.G., & Narwade M.L. (2014). Effect of temperature on chemiluminescence of luminol in aqueous ethyl amines with H_2O_2+ metal ions. *Journal of Applied Chemistry (IOSR-JAC), 7*(7), 50-52. https://doi.org/10.9790/5736-07735052

[30] Giussani, A., Farahani, P., Martínez-Muñoz, D., Lundberg, M., Lindh, R., & Roca-Sanjuán, D. (2019). Molecular basis of the chemiluminescence mechanism of luminal. *Chemistry A European Journal*, *25*(20), 5202-5213. https://doi.org/10.1002/chem.201805918

[31] Sulaiman, K.O., Onawole, A.T., Shuaib, D.T., & Saleh, T.A. (2019). Quantum chemical approach for chemiluminescence characteristics of di-substituted luminal derivatives in polar solvents. *Journal of Molecular Liquids*, *279*, 146-153. https://doi.org/10.1016/j.molliq.2019.01.110

[32] Yue, L., & Liu, Y-T. (2020). Mechanistic ınsight into pH-dependent luminol chemiluminescence in aqueous solution. *J. Phys. Chem. B*, *124*(35), 7682-7693. https://doi.org/10.1021/acs.jpcb.0c06301

[33] Moyon, N.S., Chandra, A.K., & Mitra, S. (2010). Effect of solvent hydrogen bonding on excited-state properties of luminol: A combined fluorescence and DFT study. *J. Phys. Chem. A*, *114* (1), 60-67. https://doi.org/10.1021/jp907970b

[34] Stewart, J.J.P. (1989). Optimization of parameters for semi empirical methods I. Method. *J. Comput. Chem*., *10*, 209-220. https://doi.org/10.1002/jcc.540100208

[35] Stewart, J.J.P. (1989). Optimization of parameters for semi empirical methods II. Application. *J. Comput. Chem., 10*, 221-264. https://doi.org/10.1002/jcc.540100209

[36] Leach, A.R. (1997). *Molecular modeling* (2nd ed.). Essex: Longman.

[37] Fletcher, P. (1990). *Practical methods of optimization* (1st ed.). New York: Wiley.

[38] Kohn, W., & Sham, L. (1965). Self-consistent equations including exchange and correlation effects. *J. Phys. Rev., 140*, 133-1138. https://doi.org/10.1103/PhysRev.140.A1133

[39] Parr, R.G., & Yang, W. (1989). *Density functional theory of atoms and molecules* (1st ed.). London: Oxford University Press.

[40] Cramer, C.J. (2004). *Essentials of computational chemistry* (2nd ed.). Chichester, West Sussex: Wiley.

[41] Becke, A.D. (1988). Density-functional exchange-energy approximation with correct asymptotic behavior. *Phys. Rev. A, 38*, 3098-3100. https://doi.org/10.1103/PhysRevA.38.3098

[42] Vosko, S.H., Wilk, L., & Nusair, M. (1980). Accurate spin-dependent electron liquid correlation energies for local spin density calculations: a critical analysis, *Can. J. Phys., 58*, 1200-1211. https://doi.org/10.1139/p80-159

[43] Lee, C., Yang, W., & Parr, R.G. (1988). Development of the Colle-Salvetti correlation energy formula into a functional of the electron density. *Phys. Rev., B, 37*, 785-789. https://doi.org/10.1103/PhysRevB.37.785

[44] SPARTAN 06, Wavefunction Inc., Irvine CA, USA, 2006.

[45] Gaussian 03, Frisch, M.J., Trucks, G.W., Schlegel, H.B., Scuseria, G.E., Robb, M.A., Cheeseman, J.R., Montgomery, Jr., J.A., Vreven, T., Kudin, K.N., Burant, J.C., Millam, J.M., Iyengar, S.S., Tomasi, J., Barone, V., Mennucci, B., Cossi, M., Scalmani, G., Rega, N., Petersson, G.A., Nakatsuji, H., Hada, M., Ehara, M., Toyota, K., Fukuda, R., Hasegawa, J., Ishida, M., Nakajima, T., Honda, Y., Kitao, O., Nakai, H., Klene, M., Li, X., Knox, J.E., Hratchian, H.P., Cross, J.B., Bakken, V., Adamo, C., Jaramillo, J., Gomperts, R., Stratmann, R.E., Yazyev, O., Austin, A.J., Cammi, R., Pomelli, C., Ochterski, J.W., Ayala, P.Y., Morokuma, K., Voth, G.A., Salvador, P., Dannenberg, J.J.,

Zakrzewski, V.G., Dapprich, S., Daniels, A.D., Strain, M.C., Farkas, O., Malick, D.K., Rabuck, A.D., Raghavachari, K., Foresman, J.B., Ortiz, J.V., Cui, Q., Baboul, A.G., Clifford, S., Cioslowski, J., Stefanov, B.B., Liu, G., Liashenko, A., Piskorz, P., Komaromi, I., Martin, R.L., Fox, D.J., Keith, T., Al-Laham, M.A., Peng, C.Y., Nanayakkara, A., Challacombe, M., Gill, P.M.W., Johnson, B., Chen, W., Wong, M.W., Gonzalez, C., & Pople, J.A., Gaussian, Inc., Wallingford CT, 2004.

[46] Fleming, I. (1976). *Frontier orbitals and organic reactions*. London: Wiley.